Transient Radiative Cooling of an Absorbing and Scattering Cylinder—A Separable Solution

Robert Siegel*
NASA Lewis Research Center, Cleveland, Ohio

A cylindrical region filled with absorbing-emitting material is cooled by radiation to surroundings at a much lower temperature. A solution is found showing that, for each set of parameters, the transient radial temperature distribution reaches a fixed shape, although the temperatures are decreasing with time. This "fully developed" transient region is characterized by having a constant emittance based on instantaneous values of the cylinder heat loss and mean temperature. This emittance depends only on the optical radius of the cylinder and the scattering albedo. The emittance is lower than that for a cylinder at uniform temperature. This arises from the larger local cooling and, hence, reduced temperatures of the outer layers of the cylinder. An examination of this transient emittance provides the ranges of parameters within which the simplification can be made that the cylinder has a uniform radial temperature distribution throughout the cooling process.

Nomenclature

a = absorption coefficient of absorbing-scattering region
c_p = specific heat of region
$D_n(x)$ = the function $\int_0^{\pi/2} (\cos\alpha)^{n-1} \times e^{-x/\cos\alpha} d\alpha = \int_0^1 \frac{\mu^{n-1} e^{-x/\mu}}{(1-\mu^2)^{1/2}} d\mu$
$F(r)$ = function of radius in temperature distribution
F_m = mean value of F defined in Eq. (20)
$G(r)$ = function of radius in distribution of $\tilde{I}^{1/4}$
g = function defined in Eq. (6)
I = source function in absorbing-scattering region, $\tilde{I} = \pi I/\sigma T_i^4$
i = radiation intensity
$\bar{i}$ = radiation intensity averaged over all surrounding solid angles
K_1, K_2 = integration kernels defined in Eq. (11)
K_3 = quantity defined in Eq. (23)
q_r = radiative heat flow per unit area and time
R = radial coordinate in cylinder; R_0 = outer radius
r = optical radius, $(a+\sigma_s)R$; $r_o = (a+\sigma_s)R_o$
r' = dummy variable for optical radius
T = absolute temperature, $\tilde{T} = T/T_i$
T_i = reference temperature or initial temperature
$\tilde{T}_o$ = value of $\tilde{T}$ at $r = r_o$
T_m = mean temperature of cylinder at z, Eq. (19); $\tilde{T}_m = T_m/T_i$
$\tilde{u}$ = velocity through space of cylindrical region
z = axial coordinate along length of cylinder
$\tilde{z}$ = dimensionless length, $[4z\sigma T_i^3]/\pi\tilde{u}\rho c_p R_o$
β = angle involved in cylindrical geometry, Ref. 6
$\Gamma, \Gamma^+, \Gamma^-$ = quantities defined in Eqs. (7) and (8)
ϵ_{fd} = emittance of cylinder in "fully developed" transient region based on instantaneous value of T_m
ϵ_{ut} = emittance of cylinder at uniform temperature
κ_D = optical thickness of plane layer
ρ = density of cylindrical region
σ = Stefan-Boltzmann constant
σ_s = scattering coefficient in absorbing-scattering region
τ = time
Ω = albedo for scattering, $\sigma_s/(a+\sigma_s)$

Received May 26, 1987; revision received July 27, 1987.

*Research Scientist, Office of the Chief Scientist. Member AIAA.

Introduction

THIS paper is concerned with transient cooling by radiation of energy from a region filled with an absorbing and scattering medium. The governing equations are nonlinear because the heat capacity term depends on the first power of the temperature, while the radiative terms contain temperature to the fourth power. Determining the temperature distribution requires an integration around each location in the region of the radiative contributions from the surrounding volume. The complexity of these integrations increases rapidly as the geometry is changed from a plane layer to an infinitely long cylinder and then to rectangular or other three-dimensional shapes. The solution is much more complex when the temperature distribution must be determined in contrast with having, for example, a well-mixed region at a uniform temperature. Radiation calculations are often carried out to determine performance for an assumed temperature distribution. This simplification is not possible for transient cooling studies, as the temperatures are changing throughout the process.

A particular type of solution is found here that provides a useful comparison of transient cooling, for which the temperature distribution is computed, with radiative cooling of a region at uniform temperature. During transient cooling, there are relatively low temperatures within the outer portions of the cylinder. This reduces the cylinder emittance as compared with a cylinder at uniform temperature. The reduction of emittance depends on the optical radius of the cylinder and on the amount of scattering present.

The solution obtained here applies for cooling in an environment at much lower temperature than the cylinder temperature. This was motivated by the need for radiative cooling in an outer space environment to eliminate waste heat from power conversion systems. A particular solution is obtained here by a separation-of-variables method. This type of solution was motivated by previous work in Refs. 1 and 2. In Ref. 1, a numerical solution was obtained for transient cooling of a plane layer in surroundings at zero temperature. It was

found that the layer emittance, based on instantaneous values of the heat loss and mean temperature, reached a constant value after an initial transient period. In Ref. 2, this behavior was demonstrated from the governing integral equations and it was found that, during a cooling transient, a condition is reached wherein the shape of the dimensionless radial temperature distribution does not continue to change with time. The heat loss becomes proportional to the integrated mean temperature raised to the fourth power, so that the transient emittance becomes constant. If the optical radius is small or the scattering albedo is large, the radial temperature distribution tends to be rather uniform and the transient emittance remains close to that for a uniform temperature region. The similarity solution in Ref. 2 yielded the range of optical thickness and albedo within which the emittance would deviate from the uniform temperature value. Thus, this solution can be used to determine when a detailed transient solution is necessary or if the simplifying assumption of an instantaneous uniform radial temperature distribution can be applied.

The type of solution in Ref. 2 is developed here for a cylindrical geometry. The analyses in Refs. 1 and 2 were motivated by the need for radiative dissipation of waste heat from powerplants operating in outer space. The liquid-drop radiator[3,4] has been proposed as a lightweight device that can be conveniently deployed in space. In this radiator, multiple streams of small liquid drops are passed in a directed manner through space where they cool before being collected for reuse. The streams fill an envelope that can be in the form of a plane layer. A cylindrical envelope has also been thought of as a possible configuration and some of the laboratory experiments to test the radiator concept may utilize a cylindrical shape. In addition to its possible application to liquid-drop radiator development, the present solution is of general interest in the study of radiative transfer theory.

There have been a number of significant papers in the literature on the radiative behavior of cylindrical geometries. A few of them are briefly discussed here. Two of the early papers[5,6] contain derivations of the local radiative flux and some steady-state computations. The computations are more complicated than for a plane layer, since the relations involve functions that are not tabulated. For a plane layer, the analysis contains exponential integral functions that are readily available in tabulated form or as a computer subroutine. One of the heat flux expressions from Ref. 6 will be used here. Some nongray calculations were carried out in Refs. 7 and 8 and discussions of an error and the accuracy of the radiative flux relations are in Refs. 9 and 10. The solution in Ref. 11 is for a cylindrical medium surrounding a line source of energy. Approximate solutions for emittances for cylinders and spheres are in Ref. 12, obtained by using Eddington's approximation. More recent solutions involving anisotropic scattering and heat conduction are in Refs. 13 and 14. These references are for steady temperature conditions. The present analysis will provide emittances and temperature distributions for transient behavior including scattering.

Analysis

The cylindrical region is shown in Fig. 1. With regard to applications for radiative heat dissipation in space, the region could be filled with absorbing and scattering liquid drops or particles. The cylindrical region is moving through space with a uniform velocity $\bar{u}$ and the transient cooling will be formulated as a function of distance z. By use of the transformation $\tau = z/\bar{u}$, the observer can move with the region. Hence, the solution also applies for transient cooling of a stationary cylinder; thus, it is often convenient to discuss the results in this way. The effect of the temperature of the surrounding environment is neglected; it is assumed that the space environment is at a much lower temperature than the radiating cylinder. The radiative properties are assumed to be gray. For the fluids in a liquid-drop radiator, this can be a reasonable

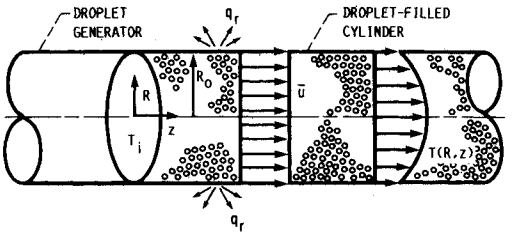

Fig. 1 Geometry of radiating cylindrical region filled with hot droplets (or particles).

approximation for the property behavior in the infrared region of interest.[4] Since the drop diameters are expected to probably be at least 50 μm, nongray wavelength interference effects within the drops are probably not significant. The scattering is assumed isotropic, which would be expected to yield reasonable results,[15] as the effects of anisotropy tend to cancel out within the region, yielding a behavior that is reasonably isotropic. Since the axial length of the radiator is orders of magnitude larger than the cross-sectional dimension, the axial radiative exchange is neglected. Heat conduction across the cylinder can be neglected for a droplet- or particle-filled region in the vacuum of outer space. The drops are collected before they are allowed to cool to their solidification temperature.

Equations for Radiative Cooling

The energy equation for transient cooling by radiation of a cylindrical region filled with an absorbing and scattering medium is given in terms of the radial radiative flux by Ref. 16 as

$$\bar{u}\rho c_p \frac{\partial T}{\partial z} = -\frac{1}{R}\frac{\partial}{\partial R}[Rq_r(R)] = -\frac{a+\sigma_s}{r}\frac{\partial}{\partial r}[rq_r(r)] \quad (1)$$

From Eqs. (14-38) in Ref. 16,

$$\frac{1}{R}\frac{\partial}{\partial R}[Rq_r(R)] = 4a(\sigma T^4 - \pi\bar{I}) \quad (2)$$

For an absorbing and scattering region, Eqs. (14-66) in Ref. 16 give

$$I = (1-\Omega)\frac{\sigma T^4}{\pi} + \Omega\bar{I} \quad (3)$$

The $\bar{I}$ is eliminated from Eqs. (1-3) to yield

$$\bar{u}\rho c_p \frac{\partial T}{\partial z} = -\frac{4\pi a}{\Omega}\left(\frac{\sigma T^4}{\pi} - I\right) \quad (4)$$

$$I = \frac{\sigma T^4}{\pi} - \frac{\Omega}{1-\Omega}\frac{1}{4\pi}\frac{1}{r}\frac{\partial}{\partial r}[rq_r(r)] \quad (5)$$

The radiative flux q_r for an infinitely long cylinder was derived by Kesten[6] in the form,

$$q_r(r) = 4\frac{r_o}{r}\int_{\beta=0}^{\sin^{-1}(r/r_o)}\left\{\int_{r'=r_o\sin\beta}^{r} D_2[\Gamma(r,r',\beta)]\frac{I(r')}{g(r',\beta)}dr' - \int_{r'=r}^{r_o} D_2[\Gamma(r',r,\beta)]\frac{I(r')}{g(r',\beta)}dr' + \int_{r'=r_o\sin\beta}^{r_o} D_2[\Gamma(r,r_o\sin\beta,\beta) + \Gamma(r',r_o\sin\beta,\beta)]\frac{I(r')}{g(r',\beta)}dr'\right\}\cos\beta\, d\beta \quad (6)$$

where

$$g(r',\beta)=\left[1-\left(\frac{r_o}{r'}\right)^2\sin^2\beta\right]^{1/2}$$

$$\Gamma(c,b,\beta)=\int_b^c\frac{d\eta}{g(\eta,\beta)}$$

$$D_n(x)=\int_0^{\pi/2}(\cos\alpha)^{n-1}e^{-x/\cos\alpha}\,d\alpha=\int_0^1\frac{\mu^{n-1}e^{-x/\mu}}{(1-\mu^2)^{1/2}}d\mu$$

By using $\mu=1/\cosh t$, $D_n(x)$ is found equal to the function $Ki_n(x)$ involving the repeated integral of the zeroth-order modified Bessel function K_o [see Eq. (11.2.10) in Ref. 17]. For uniform properties along the radiation paths, Γ can be combined with g and integrated to yield

$$\Gamma(c,b,\beta)=[c^2-(r_o\sin\beta)^2]^{1/2}-[b^2-(r_o\sin\beta)^2]^{1/2}\equiv\Gamma^-(c,b,\beta) \tag{7}$$

A convenient quantity is then defined as

$$\Gamma^+(c,b,\beta)=\Gamma^+(b,c,\beta)\equiv[c^2-(r_o\sin\beta)^2]^{1/2}+[b^2-(r_o\sin\beta)^2]^{1/2} \tag{8}$$

Then the radial heat flux $q_r(r)$ becomes

$$q_r(r)=4\frac{r_o}{r}\int_{\beta=0}^{\sin^{-1}(r/r_o)}\left\{\int_{r'=r_o\sin\beta}^{r}\times D_2[\Gamma^-(r,r',\beta)]\frac{I(r')}{g(r',\beta)}dr'-\int_{r'=r}^{r_o}D_2[\Gamma^-(r',r,\beta)]\frac{I(r')}{g(r',\beta)}dr'+\int_{r'=r_o\sin\beta}^{r_o}D_2[\Gamma^+(r,r',\beta)]\frac{I(r')}{g(r',\beta)}dr'\right\}\cos\beta\,d\beta \tag{9}$$

The order of integration is now changed by use of Fig. 2. To integrate over the required areas under the curve, the areas are now first traversed in vertical strips over β and are then summed horizontally over r'. This provides the convenient form,

$$q_r(r)=4\frac{r_o}{r}\left\{\int_{r'=0}^{r}I(r')\left[\int_{\beta=0}^{\sin^{-1}(r'/r_o)}\times\frac{D_2[\Gamma^-(r,r',\beta)]+D_2[\Gamma^+(r,r',\beta)]}{g(r',\beta)}\cos\beta\,d\beta\right]dr'+\int_{r'=r}^{r_o}I(r')\left[\int_{\beta=0}^{\sin^{-1}(r/r_o)}\times\frac{-D_2[\Gamma^-(r',r,\beta)]+D_2[\Gamma^+(r',r,\beta)]}{g(r',\beta)}\times\cos\beta\,d\beta\right]dr'\right\} \tag{10}$$

The $q_r(r)$ [Eq. (10)] is to be substituted into Eq. (5). Carrying out the differentiation with respect to r that is in Eq. (5) yields

$$-\frac{1}{r}\frac{\partial}{\partial r}[rq_r(r)]=-4\pi I(r)+4\pi\int_{r'=0}^{r}I(r')K_1(r',r)dr'+4\pi\int_{r'=r}^{r_o}I(r')K_2(r',r)dr' \tag{11}$$

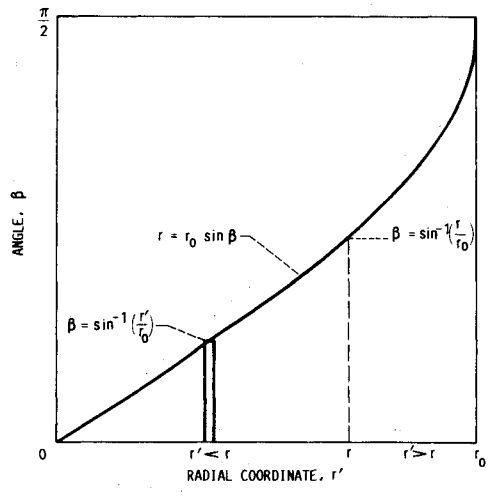

Fig. 2 Geometry used to change the order of integration.

where

$$K_1(b,c)=\frac{1}{\pi}\frac{r_o}{c}\int_{\beta=0}^{\sin^{-1}(b/r_o)}\times\frac{D_1[\Gamma^-(c,b,\beta)]+D_1[\Gamma^+(c,b,\beta)]}{g(c,\beta)g(b,\beta)}\cos\beta\,d\beta$$

$$K_2(r',r)=\frac{r'}{r}K_1(r,r')$$

Equation (11) is inserted into Eq. (5) and Eqs. (4) and (5) are then put into dimensionless form to yield

$$\frac{\partial\tilde{T}}{\partial\tilde{z}}=-\pi r_o\frac{1-\Omega}{\Omega}(\tilde{T}^4-\tilde{I}) \tag{12}$$

$$\tilde{I}=(1-\Omega)\tilde{T}^4+\Omega\left[\int_0^r\tilde{I}(r')K_1(r',r)dr'+\int_r^{r_o}\tilde{I}(r')K_2(r',r)dr'\right] \tag{13}$$

Solution by Separation of Variables

A solution is now tried in a product form with variables separated,

$$\tilde{T}(r,\tilde{z})=\tilde{T}_o(r_o,\tilde{z})F(r) \tag{14a}$$

$$\tilde{I}^{1/4}(r,\tilde{z})=\tilde{T}_o(r_o,\tilde{z})G(r) \tag{14b}$$

Substituting into Eqs. (12) and (13) yields

$$\frac{1}{\tilde{T}_o^4(r_o,\tilde{z})}\frac{d\tilde{T}_o}{d\tilde{z}}=\pi r_o\frac{1-\Omega}{\Omega}\frac{G^4(r)-F^4(r)}{F(r)} \tag{15}$$

$$G^4(r)=(1-\Omega)F^4(r)+\Omega\left[\int_0^r G^4(r')K_1(r',r)dr'+\int_r^{r_o}G^4(r')K_2(r',r)dr'\right] \tag{16}$$

Since the variables $\tilde{z}$ and r have been separated in Eq. (15), each side of this equation must be a constant. Thus, the quantity $[G^4(r)-F^4(r)]/F(r)$ must be independent of r. Equation (14a) has been defined such that $F(r_o)=1$. Then, by evaluating the quantity at $r=r_o$,

$$\frac{G^4(r)-F^4(r)}{F(r)}=G^4(r_o)-1 \tag{17}$$

A numerical solution will be used to simultaneously solve Eqs. (16) and (17) for $F(r)$ and $G(r)$.

Emittance during Transient Cooling

The emittance of the cylinder will now be obtained in two ways. The first is by taking a heat balance on an element across the entire cylinder radius and of incremental length in the z direction. This equates the convected energy within the cylinder to the radiative loss from its outer surface,

$$\pi R_o^2 \bar{u}\rho c_p \frac{\partial T_m}{\partial z} = -\epsilon_{fd}\sigma T_m^4 2\pi R_o \tag{18}$$

The mean temperature upon which ϵ_{fd} is based is given by

$$T_m(z) = \frac{2}{R_o^2}\int_0^{R_o} T(R,z)R\,dR \tag{19}$$

In dimensionless form and by use of Eq. (14a)

$$\tilde{T}_m(\tilde{z}) = \tilde{T}_o(r_o,\tilde{z})\left[\frac{2}{r_o^2}\int_0^{r_o} F(r)r\,dr\right] = \tilde{T}_o(r_o,\tilde{z})F_m \tag{20}$$

This is combined with Eq. (18) in dimensionless form to yield

$$\epsilon_{fd} = -\frac{2}{\pi}\frac{1}{\tilde{T}_o^4}\frac{d\tilde{T}_o}{d\tilde{z}}\frac{1}{F_m^3} \tag{21}$$

Substituting Eq. (15), evaluated at r_o, to eliminate $\tilde{T}_o$ gives the final form for obtaining ϵ_{fd} after F and G have been found,

$$\epsilon_{fd} = 2r_o\frac{1-\Omega}{\Omega}\frac{1}{F_m^3}[1-G^4(r_o)] \tag{22}$$

Another expression for ϵ_{fd} can be found by using the surface heat flux from Eq. (10), evaluated at $r=r_o$, in the relation $\epsilon_{fd} = q_r(r_o)/\sigma T_m^4$. I and T_m are eliminated by use of Eqs. (14b) and (20) to yield

$$\epsilon_{fd} = \frac{4}{\pi}\frac{1}{F_m^4}\int_0^{r_o} G^4(r')K_3(r',r_o)\,dr' \tag{23}$$

where

$$K_3(r',r_o) = \int_{\beta=0}^{\sin^{-1}(r'/r_o)} \times\frac{D_2[\Gamma^-(r_o,r';\beta)] + D_2[\Gamma^+(r_o,r',\beta)]}{g(r',\beta)}\cos\beta\,d\beta$$

Equations (22) and (23) were both evaluated to obtain a check on the numerical calculations.

Relations When There Is Absorption Only

For a region with absorption only ($\Omega=0$), Eqs. (15) and (16) do not yield a solution; they show only that $G(r)=F(r)$. To obtain a solution, Eq. (13) is first rearranged into the form

$$-(\tilde{T}^4-\tilde{I})\frac{1-\Omega}{\Omega} = \int_0^r \tilde{I}(r')K_1(r',r)\,dr' + \int_r^{r_o}\tilde{I}(r')K_2(r',r)\,dr' - \tilde{I} \tag{24}$$

This is substituted into Eq. (12) to eliminate Ω, which gives

$$\frac{1}{\pi r_o}\frac{\partial\tilde{I}}{\partial\tilde{z}} = \int_0^r \tilde{I}(r')K_1(r',r)\,dr' + \int_r^{r_o}\tilde{I}(r')K_2(r',r)\,dr' - \tilde{I} \tag{25}$$

The trial solution [Eqs. (14)] is now substituted: then, for $\Omega=0$, the relation is used so that $G(r)=F(r)$. This yields the following equation where the variables in $\tilde{z}$ are separated:

$$\frac{1}{\pi r_o}\frac{1}{\tilde{T}_o^4}\frac{dT_o}{d\tilde{z}} = \frac{1}{F(r)}\left[\int_0^r F^4(r')K_1(r',r)\,dr' + \int_r^{r_o} F^4(r')K_2(r',r)\,dr' - F^4(r)\right] \tag{26}$$

Since each side of this equation must be constant, the right side must be independent of r, so it is equated to itself evaluated at $r=r_o$ and the relation $F(r_o)=1$ is used. This yields an integral equation for $F(r)$,

$$F^4(r) = F(r)\left[1-\int_0^{r_o} F^4(r')K_1(r',r_o)\,dr'\right] + \int_0^r F^4(r')K_1(r',r)\,dr' + \int_r^{r_o} F^4(r')K_2(r',r)\,dr' \tag{27}$$

Since $G(r)=F(r)$ for $\Omega=0$, when there is absorption only, ϵ_{fd} is obtained from Eq. (23) with $G^4(r')$ replaced by $F^4(r')$, as found from Eq. (27).

Emittance for Cylinder at Uniform Temperature

To compare with the transient results, the emittance was obtained for a cylinder at a uniform temperature T_i. The $\tilde{I}$ for an absorbing-scattering region is found from Eq. (13), with $\tilde{T}=1$ for the uniform temperature case,

$$\tilde{I} = 1-\Omega+\Omega\left[\int_0^r \tilde{I}(r')K_1(r',r)\,dr' + \int_r^{r_o}\tilde{I}(r')K_2(r',r)\,dr'\right] \tag{28}$$

Then, by use of q_r from Eq. (10) evaluated at $r=r_o$, the emittance for uniform temperature is

$$\epsilon_{ut} = \frac{q_r(r_o)}{\sigma T_i^4} = \frac{4}{\pi}\int_{r'=0}^{r_o}\tilde{I}(r')K_3(r',r_o)\,dr' \tag{29}$$

If there is no scattering, then $\tilde{I}(r') = \tilde{T}_i^4$ and, for a uniform temperature, $\tilde{T}_i=1$, so that

$$\epsilon_{ut} = \frac{4}{\pi}\int_0^{r_o} K_3(r',r_o)\,dr' \tag{30}$$

This can be integrated to yield

$$\epsilon_{ut} = \frac{4}{\pi}\left[\int_{\beta=0}^{\sin^{-1}(r'/r_o)}\{D_3[\Gamma^-(r_o,r',\beta)] - D_3[\Gamma^+(r_o,r',\beta)]\}\cos\beta\,d\beta\right]_{r'=0}^{r_o}$$

Since $\Gamma^-(r_o,r_o,\beta)=0$, $D_3(0)=\pi/4$, and $\Gamma^+(r_o,r_o,\beta)=2r_o\cos\beta$, this becomes

$$\epsilon_{ut} = 1-\frac{4}{\pi}\int_0^{\pi/2} D_3(2r_o\cos\beta)\cos\beta\,d\beta \tag{31}$$

For an optically thin cylinder, this can be further reduced. The D_3 for small arguments is found from Ref. 18 as $D_3(\xi) = \pi/4-\xi+\ldots$. Then, for $r_o \ll 1$, ϵ_{ut} becomes

$$\epsilon_{ut} = 1-\frac{4}{\pi}\int_0^{\pi/2}\left(\frac{\pi}{4}-2r_o\cos\beta\right)\cos\beta\,d\beta = 2r_o \tag{32}$$

This agrees with Eq. (17-53) in Eq. 16.

Numerical Solution

For $\Omega>0$, Eqs. (16) and (17) were solved numerically for $F^4(r)$ and $G^4(r)$ at uniformly spaced r values between 0 and r_o. To carry out the integrations, spline fits were made of the F^4 and G^4 distributions. The spline coefficients were used to interpolate values at locations between the grid points for use in a Gaussian integration subroutine. The number of integration points was usually several times larger than the number of grid points. An iterative solution method was used and, in most instances, the calculations were started using $F=G=1$ as initial trial solutions. After converged results were obtained, corresponding to some values of the parameters, the iterations could be started using approximate radial distributions of F and G closer to the expected final results. The initial functions were inserted into the right side of Eq. (16). After integrating, the difference between the right side and the trial $G^4(r)$ was multiplied by an acceleration factor such as 1.5 and the results were added to the trial $G^4(r)$ to obtain a new $G^4(r)$ with which to continue the iteration of Eq. (16). After a few iterations, $F(r)$ was obtained from Eq. (17) by using Newton's method to solve this nonlinear equation. $F(r)$ was then used in Eq. (16) to carry out a few more iterations on $G^4(r)$. After convergence to within a small relative change of about 10^{-3}, the acceleration factor on G^4 was decreased to 1.2 and Eq. (16) was iterated to a convergence of 5×10^{-5} before $F(r)$ was obtained. This procedure was continued until both $G^4(r)$ and $F(r)$ were converged within this maximum relative change for an iteration. The calculations were checked by reducing the size of Δr. Several cases were carried out using 10, 20, and 40 Δr intervals between $r=0$ and r_o; 10 to 20 increments were usually sufficient. When $\Omega=0$, Eq. (27) was solved in a similar manner, using an acceleration factor of 1.2 on $F^4(r)$ and obtaining convergence of F^4 to within a relative change of 5×10^{-5}. Most cases required several minutes of running time on an IBM 370 computer.

The solution of Eq. (16) requires the evaluation of the integration kernels $K_1(r',r)$ and $K_2(r',r)$. These functions are shown in Fig. 3 for $r_o=0.5$ and 5. $K_2(r',0)$ is an exception, as it reaches a finite limit of $\pi/2$ as $r'\to0$. By taking the limit,

$$\lim_{r\to0} K_2(r',r)$$

it is found that $K_2(r',0)=D_1(r')$. The other values of the kernel all become infinite as $r'\to r$; thus, the integations in Eq. (16) must be given special consideration as the singular point is approached. The kernels can be integrated analytically to obtain

$$\int K_1(r',r)\,dr' = \frac{1}{\pi}\frac{r_o}{r}\int_{\beta=0}^{\sin^{-1}(r'/r_o)} \times \frac{D_2[\Gamma^-(r,r',\beta)]-D_2[\Gamma^+(r,r',\beta)]}{g(r,\beta)}\cos\beta\,d\beta \qquad (33a)$$

$$\int K_2(r',r)\,dr' = -\frac{1}{\pi}\frac{r_o}{r}\int_{\beta=0}^{\sin^{-1}(r/r_o)} \times \frac{D_2[\Gamma^-(r,',r\beta)]+D_2[\Gamma^+(r,r',\beta)]}{g(r,\beta)}\cos\beta\,d\beta \qquad (33b)$$

The integrations in Eq. (16) can thus be performed analytically for a small region adjacent to the singularity, with F and G each kept constant within this small region. The numerical results were checked by reducing the size of this region to be sure its size had no effect.

To illustrate the evaluation of the kernels, $K_1(r',r)$ will be discussed as an example. From the K_1 expression in Eq. (11) and by using the definition of D_1, K_1 requires a double integration for its evaluation

$$K_1(r',r)=\frac{1}{\pi}\frac{r_o}{r}\int_{\beta=0}^{\sin^{-1}(r'/r_o)} \times \frac{\int_0^1[e^{-\Gamma^-(r,r',\beta)/\mu}+e^{-\Gamma^+(r,r',\beta)/\mu}][1/(1-\mu^2)^{1/2}]d\mu}{[1-(r_o/r)^2\sin^2\beta]^{1/2}\,[1-(r_o/r')^2\sin^2\beta]^{1/2}\cos\beta\,d\beta} \qquad (34)$$

If we let $\xi=(r_o/r')\sin\beta$, Eq. (34) transforms to

$$K_1(r',r)=\frac{r'}{\pi}\int_{\xi=0}^1\int_{\mu=0}^1 \times \frac{e^{-\Gamma^-(r,r',\beta)/\mu}+e^{-\Gamma^+(r,r',\beta)/\mu}}{[(1-\mu^2)(r^2-r'^2\xi^2)(1-\xi^2)]^{1/2}}d\mu\,d\xi \qquad (35)$$

Equation (35) shows that there are square root singularities in both μ and ξ. The integrations were performed with Gaussian integration routines having weighting factors for a square root singularity. Three routines were tried with either 9, 20, or 48 weighting factors. More factors were needed as r_o increased, since K_1 has a sharper increase near the singularity. This is shown by comparing the two parts of Fig. 3. Twenty weights were usually sufficient for the present calculations extending to $r_o=7$. The same type of procedure was used to evaluate Eqs. (33). As a check on the integration method, D_1, D_2, and D_3 were also evaluated and the results agreed with those in Ref. 18. D_3 values were used in Eq. (31).

Results and Discussion

Using the numerical procedures described in the analysis, Eqs. (15) and (16) were solved to obtain $F(r)$ and $G(r)$ for several values of r_o and Ω with $\Omega>0$. When $\Omega=0$, Eq. (27) was solved. The emittance values were obtained from Eqs. (22) and (23) for $\Omega>0$ and from Eq. (23), with $G(r)$ replaced by $F(r)$ when $\Omega=0$. The two relations in Eqs. (22) and (23) can be shown analytically to be equal. The relation in Eq. (23) was

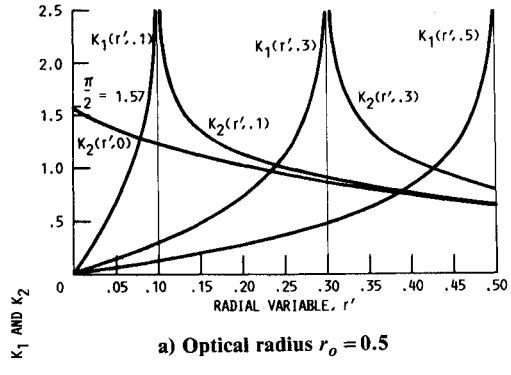

a) Optical radius $r_o=0.5$

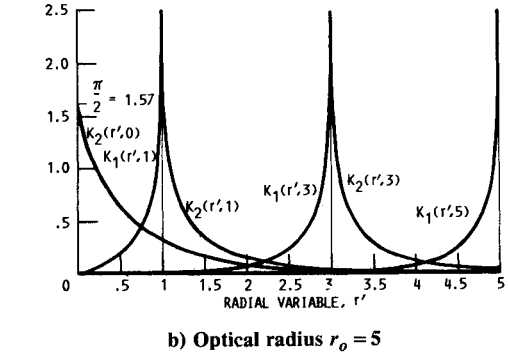

b) Optical radius $r_o=5$

Fig. 3 Kernel functions in radiative integral equation for a cylinder.

Table 1 Values of fully developed and uniform temperature emittances for transient cooling of a cylinder

Optical radius r_o		Scattering albedo Ω 0	0.3	0.6	0.8	0.9	0.95	0.98
0.5	ϵ_{fd}	0.592	0.472	0.313	0.175	0.093	0.048	0.020
	ϵ_{ut}	0.596	0.474	0.314	0.176	0.094	0.048	0.020
1	ϵ_{fd}	0.792	0.677	0.495	0.305	0.172	0.092	0.039
	ϵ_{ut}	0.814	0.689	0.500	0.306	0.173	0.092	0.039
2	ϵ_{fd}	0.850	0.778	0.643	0.457	0.290	0.168	0.074
	ϵ_{ut}	0.946	0.841	0.670	0.465	0.292	0.168	0.074
3	ϵ_{fd}	0.792	0.746	0.657	0.514	0.358	0.223	0.105
	ϵ_{ut}	0.977	0.882	0.729	0.539	0.364	0.224	0.105
4	ϵ_{fd}	0.720	0.687	0.627	0.521	0.390	0.260	0.130
	ϵ_{ut}	0.987	0.897	0.752	0.574	0.406	0.263	0.130
5	ϵ_{fd}	0.648	0.627	0.585	0.507	0.402	0.283	0.151
	ϵ_{ut}	0.992	0.904	0.764	0.593	0.432	0.291	0.151
6	ϵ_{fd}	0.587	0.572	0.542	0.483	0.398	0.294	0.165
	ϵ_{ut}	0.994	0.907	0.769	0.602	0.446	0.309	0.167
7	ϵ_{fd}	0.535	0.524	0.501	0.456	0.387	0.298	0.176
	ϵ_{ut}	0.995	0.909	0.772	0.607	0.454	0.321	0.180

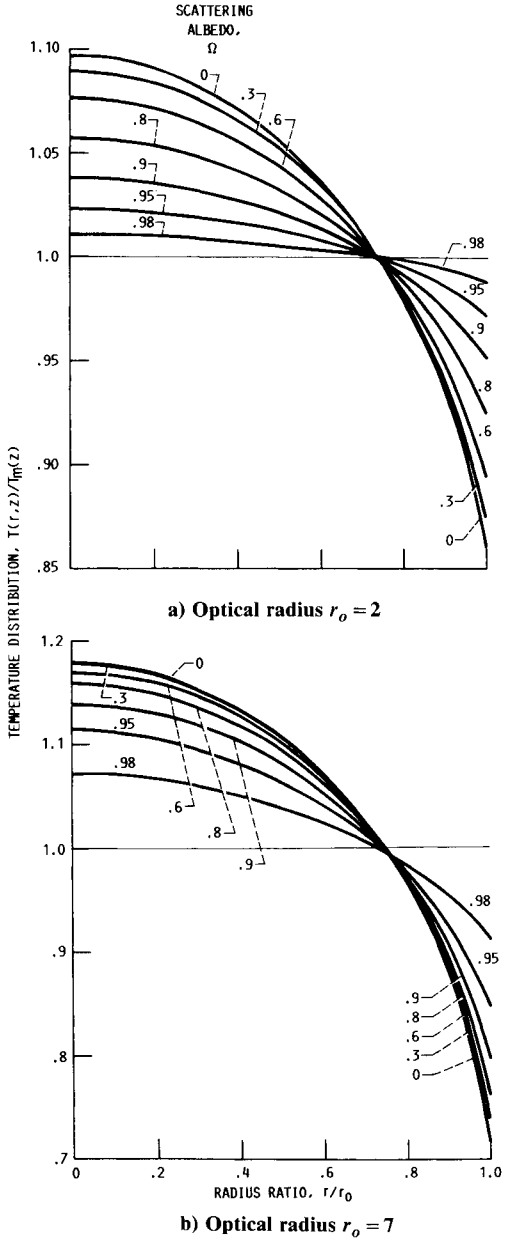

Fig. 4 Temperature distributions for fully developed transient cooling.

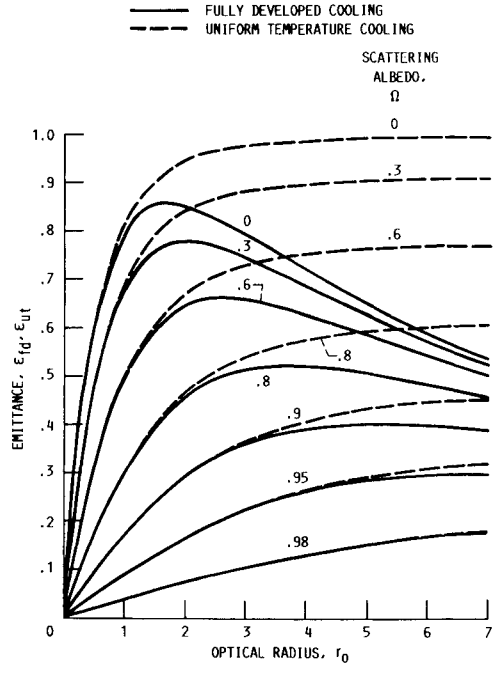

Fig. 5 Comparison of emittances for cylinder for fully developed temperature distribution and uniform temperature distribution.

found to be a little easier to evaluate accurately and, by using 10 radial increments and 20 Gaussian points in the integrations having square root singularities, the results from Eq. (23) were very close to the values obtained when using more grid points and weighting factors. By using 20 or 40 radial increments and 20 or 48 Gaussian points, depending on the value of r_o, the results from Eq. (22) came within 1% of Eq. (23), while the results from Eq. (23) changed very little.

For comparison with the emittance values for fully developed transient cooling ϵ_{fd}, the emittances were obtained for a cylinder maintained at uniform temperature ϵ_{ut}. As shown in the analysis for $\Omega > 0$, these values were calculated by solving Eq. (28) and using the resulting $\tilde{I}(r)$ in Eq. (30). For $\Omega = 0$, Eq. (31) was used.

Figure 4 shows the normalized temperature variations in the radial direction, $T(r,z)/T_m(z) = F(r)/F_m$. These distributions exist in the fully developed transient region being analyzed here, within which the separation of variables solution applies. The two parts of the figure are for different optical radii, $r_o = 2$ and 7, and they display the typical behavior of the

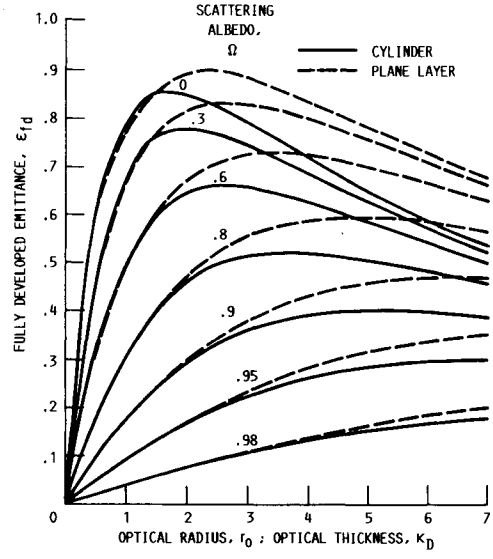

Fig. 6 Comparison of emittances of cylinder and plane layer for transient cooling in fully developed region.

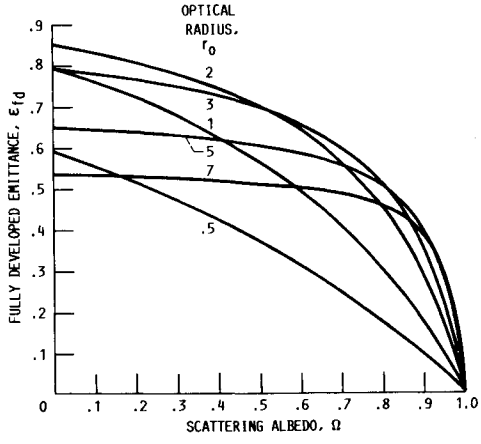

Fig. 7 Emittance of absorbing-scattering cylinder in fully developed transient region.

solutions to the integral equations. It is noted that the ordinate scale for $r_o = 7$ is somewhat larger than for $r_o = 2$; as expected, the amplitude of the temperature distribution increases as the optical radius of the cylinder increases. The temperature distributions become more uniform as the scattering is increased. This arises from the redistribution of energy across the cylinder radius that the scattering provides. As optical thickness is increased, a larger amount of scattering is required to achieve the same effect; for example, increasing Ω from 0 to 0.98 has a more significant effect in Fig. 4a than in Fig. 4b.

The emittance values are given in Table 1 for both fully developed transient cooling ϵ_{fd} and a cylinder at uniform temperature ϵ_{ut}. Results are given for various optical radii and values of the scattering albedo. Emittance curves are given in Figs. 5–7 where various comparisons are made, as will now be discussed.

Figure 5 shows how the emittance varies with optical radius while the scattering albedo is held constant for each curve. For small optical thicknesses, ϵ_{fd} increases with r_o. For each Ω, a maximum ϵ_{fd} is reached and then ϵ_{fd} decreases as the optical thickness is further increased. For zero scattering, the maximum ϵ_{fd} is at an optical radius of about 1.7. As scattering is increased, the maximum ϵ_{fd} occurs at increasingly larger values of r_o. For $\Omega = 0.98$, the maximum is at $r_o > 7$ and hence it does not appear on the figure. For comparison, the values of ϵ_{ut} are shown for a cylinder at uniform temperature. In this instance, the emittance curve for each Ω increases continuously with optical radius. For $\Omega = 0$, the cylinder radiates essentially like a blackbody when r_o is greater than about 5. For each Ω value greater than zero, the curve of ϵ_{ut} increases toward a different constant value; this asymptotic value decreases as Ω increases.

For small optical radii (optically thin cylinders), the transient temperature distribution tends to be uniform; so the two sets of curves coincide for small r_o. As the scattering is increased, the curves coincide over a larger range of r_o, since the scattering tends to equalize the temperature distribution, as shown in Fig. 5. For $\Omega = 0.98$, the curves for ϵ_{fd} and ϵ_{ut} are practically the same all the way out to $r_o = 7$. For Ω less than 0.8, there is a very significant difference between ϵ_{fd} and ϵ_{ut} when the cylinder is not optically thin. This is the result of the cooling of the outer regions of the cylinder, which decreases its emissive ability because of its relatively cool outer layers.

An important use of Fig. 5 is that it shows when the simplifying assumption of a uniform temperature region can be used with acceptable accuracy for a transient calculation of heat loss. For Ω near zero, this simplifying assumption would be good for r_o exending to only a little above unity. For larger scattering, for example $\Omega = 0.8$, the assumption could be used for values of r_o up to about 3. The results also show the lower limit that the emittance can reach during the transient cooling process. For a plane layer initially at uniform temperature,[1] the ϵ_{fd} value was reached after about 30% of the energy had been radiated away; this was true for all optical thicknesses and values of the scattering albedo. Some preliminary work on the transient cooling of a cylinder from an initially uniform temperature indicates that the 30% value is probably a good approximation.

Figure 6 provides a comparison of the emittance of a cylinder and a plane layer for transient cooling in the fully developed region. The plane layer results from Ref. 2 form one set of curves for various Ω values. For optically thin regions at uniform temperature, theory[16] shows that a cylinder will have an emittance very close to that of a plane layer if the optical radius of the cylinder is equal to the optical thickness of the plane layer, $r_o = \kappa_D$. For small r_o and κ_D, the temperature distributions remain practically uniform during transient cooling; hence, the two sets of curves in Fig. 6 are in good agreement for small values of the abscissa. At larger optical thicknesses, the values for a cylinder fall significantly below the values for a plane layer. As the scattering is increased, the results for the cylinder and the plane layer agree out to larger values of the optical thickness.

The ϵ_{fd} for the cylinder is plotted in Fig. 7 as a function of Ω for constant values of r_o in the range 0.5–7. For each r_o, the ϵ_{fd} decreases as Ω is increased. For a cylinder that is fairly thin optically ($r_o = 0.5$), ϵ_{fd} has a rather uniformly decreasing trend as Ω increases, although the rate of decrease increases somewhat with Ω. In the range of $r_o = 1$ and 2, ϵ_{fd} increases with optical radius and the curves for a fixed r_o decrease more slowly for small Ω. For larger r_o, the cooling in the outer layers of the cylinder becomes important and ϵ_{fd} decreases as r_o is increased, unless the scattering is large. The equalization of the temperature distribution by large Ω results in ϵ_{fd} increasing with r_o for large Ω. For large r_o, such as $r_o = 7$, ϵ_{fd} remains fairly uniform as Ω increases from zero; then, ϵ_{fd} decreases rapidly to zero as Ω approaches unity.

Conclusions

A separation of variables solution was obtained for the transient cooling of a cylindrical region losing heat by radiation to surroundings at a much lower temperature. The solution is valid for a "fully developed" transient region wherein the radial temperature distribution reaches a shape that does not change during the remainder of the cooling process, while the temperature level continues to decrease. Throughout the fully developed cooling period, the emittance of the cylinder remains constant when based on the instantaneous heat loss and integrated mean temperature. This behavior is shown to

exist from the governing energy relations for an absorbing-scattering medium. The stronger cooling of the outer regions of the cylinder results in outer temperatures lower than the mean temperature. This causes the transient emittance of the cylinder to be below that for a cylinder at uniform temperature. The transient emittance values, and the corresponding values for a cylinder at uniform temperature, provide the range of possible emittances during transient cooling from an initially uniform temperature condition. Thus, the results show under what conditions of optical radius and scattering albedo the uniform temperature approximation can be used with reasonable accuracy as a simplification during transient radiative cooling.

References

[1]Siegel, R., "Transient Radiative Cooling of a Droplet-Filled Layer," *Journal of Heat Transfer,* Vol. 109, No. 1, Feb. 1987, pp. 159-164.

[2]Siegel, R., "Separation of Variables Solution for Nonlinear Radiative Cooling," *International Journal of Heat and Mass Transfer,* Vol. 30, No. 5, 1987, pp. 959-965.

[3]Mattick, A.T. and Hertzberg, A., "Liquid Droplet Radiators for Heat Rejection in Space," *Journal of Energy,* Vol. 5, Nov.-Dec. 1981, pp. 387-393.

[4]Presler, A.F., Coles, C.E., Diem-Kirsop, P.S., and White, K.A., "Liquid Droplet Radiator Program at the NASA Lewis Research Center," ASME Paper 86-HT-15, June 1986.

[5]Heaslet, M.A. and Warming, R.F., "Theoretical Predictions of Radiative Transfer in a Homogeneous Cylindrical Medium," *Journal of Quantitative Spectroscopy and Radiative Transfer,* Vol. 6, Nov.-Dec. 1966, pp. 751-774.

[6]Kesten, A.S., "Radiant Heat Flux Distribution in a Cylindrically-Symmetric Nonisothermal Gas with Temperature-Dependent Absorption Coefficient," *Journal of Quantitative Spectroscopy and Radiative Transfer,* Vol. 8, Jan. 1968, pp. 419-434.

[7]Habib, I.S. and Greif, R., "Nongray Radiative Transport in a Cylindrical Medium," *Journal of Heat Transfer,* Vol. 92, No. 1, Feb. 1970, pp. 28-32.

[8]Wassel, A.T. and Edwards, D.K., "Molecular Gas Band Radiation in Cylinders," *Journal of Heat Transfer,* Vol. 96, No. 1, Feb. 1974, pp. 21-26.

[9]Chiba, Z. and Greif, R., Discussion of "Nongray Radiative Transport in a Cylindrical Medium," *Journal of Heat Transfer,* Vol. 95, No. 1, Feb. 1973, p. 142.

[10]Edwards, D.K. and Wassel, A.T., "The Radial Radiative Heat Flux in a Cylinder," *Journal of Heat Transfer,* Vol. 95, No. 2, May 1973, pp. 276-277.

[11]Schmid-Burgk, J., "Radiant Heat Flow Through Cylindrically-Symmetric Media," *Journal of Quantitative Spectroscopy and Radiative Transfer,* Vol. 14, Oct. 1974, pp. 979-987.

[12]Adzerikho, K.S. and Nekrasov, V.P., "Luminescence Characteristics of Cylindrical and Spherical Light-Scattering Media," *International Journal of Heat and Mass Transfer,* Vol. 18, Oct. 1975, pp. 1131-1138.

[13]Azad, F.H. and Modest, M.F., "Evaluation of the Radiative Heat Flux in Absorbing, Emitting and Linear-Anisotropically Scattering Cylindrical Media," *Journal of Heat Transfer,* Vol. 103, No. 2, May 1981, pp. 350-356.

[14]Fernandes, R. and Francis, J., "Combined Conductive and Radiative Heat Transfer in an Absorbing, Emitting, and Scattering Cylindrical Medium," *Journal of Heat Transfer,* Vol. 104, No. 4, Nov. 1982, pp. 594-601.

[15]Stockham, L.W. and Love, T.J., "Radiative Heat Transfer from a Cylindrical Cloud of Particles," *AIAA Journal,* Vol. 6, Oct. 1968, pp. 1935-1940.

[16]Siegel, R. and Howell, J.R., *Thermal Radiation Heat Transfer,* 2nd ed., Hemisphere Publishing, Washington, DC, 1981.

[17]Abramowitz, M. and Stegun, I.A. (eds.), *Handbook of Mathematical Functions,* NBS Applied Mathematics Series, No. 55, Nov. 1967.

[18]Yuen, W.W. and Wong, L.W., "Numerical Computation of an Important Integral Function in Two-Dimensional Radiative Transfer," *Journal of Quantitative Spectroscopy and Radiative Transfer,* Vol. 29, Feb. 1983, pp. 145-149.